Acta Biochim Biophys Sin, 2016, 48(2), 153–160
doi: 10.1093/abbs/gmv124
Advance Access Publication Date: 11 January 2016
Original Article

Original Article

Triticumoside induces apoptosis via caspase-dependent mitochondrial pathway and inhibits migration through downregulation of MMP2/9 in human lung cancer cells

Barun Poudel[1,†], Hyeon-Hui Ki[1,†], Bui Thi Thuy Luyen[2], Young-Mi Lee[3], Young-Ho Kim[2], and Dae-Ki Kim[1,*]

[1]Department of Immunology and Institute for Medical Sciences, Chonbuk National University Medical School, Jeonju, Jeonbuk 561-756, Korea, [2]College of Pharmacy, Chungnam National University, Daejeon 305-764, Korea, and [3]Department of Oriental Pharmacy, College of Pharmacy and Wonkwang-Oriental Medicines Research Institute, Wonkwang University, Iksan, Jeonbuk 570-749, Korea

[†]These authors contributed equally to this work.
*Correspondence address. Tel: +82-632703080; Fax: +82-638556807; E-mail: daekim@jbnu.ac.kr

Received 25 June 2015; Accepted 8 October 2015

Abstract

Non-small cell lung cancer (NSCLC) is the major cancer-related death worldwide with only 14% five-year survival rate. Triticumoside, a phenolic compound present in *Triticum aestivum* sprout extract, has been recognized to have antiobesity and anti-inflammatory effects. However, the effect of triticumoside on cancer cell proliferation and migration has not been studied. In order to elucidate whether triticumoside exhibits an anticancer effect, cells were incubated with different doses of triticumoside, and apoptosis was assessed by observing cell viability, cellular morphological changes, and annexin-V-fluorescein isothiocyanate/propidium iodide staining. Cell cycle analysis, western blotting, wound healing assay, and quantitative-polymerase chain reaction were also performed. Triticumoside exhibited marked cytotoxicity in the cells in dose- and time-dependent manner. Triticumoside caused morphological changes, including cellular rounding, nuclear condensation, and shrinkage. Likewise, triticumoside enhanced the sub-G1 proportion of cells. Additionally, triticumoside regulated expression of apoptosis-associated proteins, such as B-cell lymphoma 2 (Bcl-2), Bcl-2-associated X, and procaspase-3/9. Triticumoside also inhibited migration of the cells through downregulation of matrix metalloproteinase-2/9 (MMP2/9). Collectively, these results suggest that triticumoside induces apoptosis through caspase-dependent mitochondrial pathway and suppresses migration via inhibition of MMP2/9 in NSCLC A549 cells.

Key words: triticumoside, lung cancer, apoptosis, migration, *Triticum aestivum*

Introduction

Lung cancer is the major cause of cancer-related death worldwide and 80% of them are non-small cell lung cancer (NSCLC) cases. NSCLC patients show only 14% five-year survival rate [1]. The reason behind the poor survival rate is that the most of the lung cancer patients with late-stage disease are not curable by current therapeutic strategies. Many new therapeutic agents that improve surgical techniques and cause increased use of chemoradiotherapy for locally advanced lung cancer have been proposed. However, the results showed that they are not effective. Thus, effective diagnosis and

identification of effective molecular therapeutic agents are required to treat lung cancer [2].

Triticum aestivum (TA), commonly called as wheat, is one of the cereal grain cultivated worldwide. During germination and sprouting, many useful phenolic compounds occur in seeds of TA. The germinated wheat leaves are consumed as a rich source of soluble fibers, minerals, vitamins, and antioxidants [3]. Previous reports have indicated that extract of TA has antidiabetic, antihyperlipidemic, and anticancer effects [4–9]. Moreover, TA extract is known to contain several phytocompounds such as leuteolin, isoscoparin, isoorientin, and triticumoside [10–12]. However, there have not yet been any studies on the effects and potential mechanisms of anticancer effects of compounds isolated from TA, until now.

This study was performed to evaluate the anticancer effects of the phenolic compound, triticumoside, purified from TA in NSCLC A549 cells. Furthermore, we aimed to elucidate the underlying mechanisms associated with its anticancer effects. Results demonstrated that triticumoside causes apoptosis via the mitochondria-dependent pathway, and inhibits cell growth and migration. Triticumoside-mediated inhibition of cell migration was due to reduced matrix metalloproteinase-2/9 (MMP2/9) expression. Additionally, triticumoside treatment increased the percentage of cells in sub-G1 stage. Furthermore, triticumoside treatment significantly increased the expression of Bcl-2-associated X (Bax), while significantly decreased the expressions of B-cell lymphoma 2 (Bcl-2) and procaspase-3/9, which suggests that the cytotoxicity on A549 cells was caused by cell cycle arrest and apoptosis. These results suggest that triticumoside exerts apoptosis and diminishes migration of A549 cells, and triticumoside may be used as a potential anti-lung cancer drug.

Materials and Methods

Materials and reagents

Dimethyl sulfoxide (DMSO), 4′,6-diamidino-2-phenylindole (DAPI), and propidium iodide (PI) were purchased from Sigma (St Louis, USA). Dulbecco's modified Eagle's medium (DMEM) and fetal bovine serum (FBS) were from Hyclone (Logan, USA). TRIzol reagent and SuperScript III kit were obtained from Invitrogen Life Technologies (Carlsbad, USA). Cell counting kit-8 (CCK-8) was purchased from Dojindo Molecular Technologies (Rockville, USA). Anti-Bax (sc-6236), anti-procaspase-3 (sc-7148), anti-procaspase-9 (sc-8355), anti-β-actin (sc-47778) antibodies, rabbit and mouse secondary antibodies, and protein assay kit (RIPA buffer) were obtained from Santa Cruz Biotechnology (Santa Cruz, USA). Annexin-V-fluorescein isothiocyanate (FITC) staining antibody was obtained from Biolegend (San Diego, USA). Anti-Bcl-2 antibody (BS 1511) was purchased from Bioworld Technologies (St Louis Park, USA). The caspase-3 inhibitor (Z-DEVD; FMK004) and caspase-9 inhibitor (Z-LEHD; FMK008) were obtained from R&D Systems, Inc. (Minneapolis, USA). Curcumin (C7727) was obtained from Sigma.

Extraction and purification of triticumoside from TA

Triticumoside was prepared as previously described [10,12]. Briefly, methanol extract of TA sprouts was partitioned with *n*-hexane, dichloromethane (CH_2Cl_2), ethyl acetate (EtOAc), and *n*-BuOH to give hexane extract, CH_2Cl_2 extract, EtOAc extract, BuOH extract, and water layer, respectively. EtOAc and BuOH extracts were combined and fractionated on a silica gel column eluting with $CHCl_3$/MeOH (5/1, v/v), a YMC column eluting with MeOH/H_2O (1/1, v/v), and further purified on a silica gel column chromatography with CH_2Cl_2/MeOH (6/1, v/v) as eluent to yield triticumoside (**Fig. 1**).

Cell culture

Human NSCLC A549 and HEK293 cell lines were from American Type Culture Collection (Manassas, USA). Calu-6 lung cancer cells were generous gift of Professor Woo Hyun Park (Chonbuk National University, Jeonju, Korea). Cells were grown in DMEM containing 10% FBS and 100 U/ml penicillin/streptomycin sulfate (Welgene, Seoul, Korea). Cells were incubated in humidified 5% CO_2 atmosphere at 37°C. Triticumoside was dissolved in 0.01% DMSO. DMSO (0.01%) did not affect A549 cells and was used as vehicle.

Cell viability

The cells were treated with mentioned doses of triticumoside for indicated time, and cell viability was measured using CCK-8, according to the manufacturer's recommendations. Absorbance was measured at 450 nm on a microplate reader (Anthos Labtec Instruments GmbH, Salzburg, Austria).

Real-time polymerase chain reaction

Total RNA was extracted using TRIzol reagent, according to the manufacturer's protocol. And 2 μg RNA was used for cDNA synthesis using Super Script™ III kit. Then mRNA expression was quantitatively determined by ABI Real-Time polymerase chain reaction (PCR) system from Applied Biosystem Inc. (Forster City, USA) using SYBR

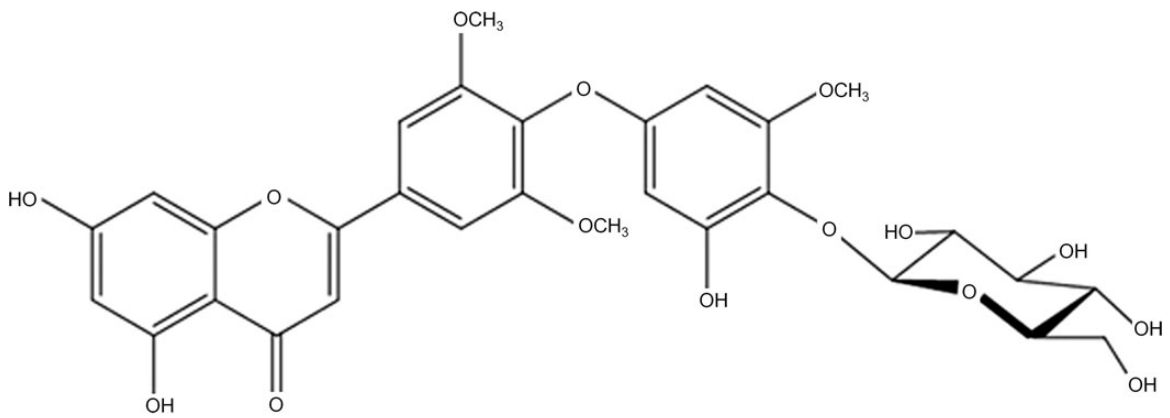

Figure 1. Chemical structure of triticumoside

Green PCR Master Mix (Invitrogen). GAPDH was the invariant control. The specific primers for the genes are listed in Table 1. Results were expressed as relative expression to that of control.

Migration assay

Migration assay was performed using 35 mm μ-dish culture inserts (Ibidi, Martinsried, Germany), according to manufacturer's recommendations. Briefly, cells were cultured in complete medium in the inserts and left for confluency (>90%). After 16 h, inserts were detached and cells were washed two times with phosphate buffered saline (PBS) to remove the cellular debris in order to yield an accelular line per well. To initiate migration, cells were treated with or without triticumoside in the medium. Cells were then allowed to migrate during 18-h incubation. At 0 and 18 h, cells were photographed with an Olympus IX71 microscope (Olympus Optical Co., Ltd, Tokyo, Japan), and distance of the migrated cells' margin was measured using I'MEASURE software (INGPLUS Co., Ltd, Seoul, Korea).

DAPI and phase contrast microscopy

Cells were cultured at 1×10^5 cells/well in 48-well plates. After overnight incubation, cells were treated with or without indicated doses of triticumoside and further incubated for 48 h. Then, cells were washed two times with PBS, and phase contrast microscopy was performed. Then, cells were fixed with 3% paraformaldehyde for 10 min, washed with PBS, and permeabilized with 0.1% Triton-X for 5 min. After this, cells were rinsed with PBS, and covered with 1 μg/ml DAPI in PBS at dark for 5 min. Cells were washed three times with PBS and were visualized by fluorescence microscopy.

Annexin-V FITC PI staining

A549 cells were cultured in 6-well cell culture plates and incubated in 5% CO_2 at 37°C for 24 h. Triticumoside was diluted to the desired concentrations with culture medium and added to each well. Cell culture was continued for 48 h at 37°C, 5% CO_2, and 1×10^5 cells were collected, centrifuged at 400 *g* for 5 min, and resuspended in 100 μl of binding buffer. Annexin V-FITC (5 μl) was added and mixed. After the addition of 5 μl of PI staining solution, the cells were incubated for 15 min in the dark at room temperature, 400 μl of binding buffer was added, and the cells were analyzed using a FACSort Becton Dickinson Flow Cytometer to detect cell apoptosis.

Cell cycle analysis

The suspended single cell solutions treated with triticumoside at indicated concentrations for 24 h were harvested, washed with PBS, and fixed with 70% ethanol overnight at −20°C. Then, the cells were washed with PBS again and treated with 100 μl of 100 mg/l PI at 4°C for 20 min in the dark. Finally, cells were assayed using the flow cytometer at 488 nm, and data were analyzed with FlowJo software (Tree Star, Inc., Ashland, USA). For each sample, 10 000 cells were analyzed.

Western blot analysis

Cells were lysed in ice-cold RIPA buffer for 40 min and centrifuged (12,000 *g*) for 20 min at 4°C. Protein concentration was measured using a bicinchoninic acid method. Thirty micrograms of lysates were subject to 8% sodium dodecyl sulfate-polyacrylamide gel electrophoresis and transferred to polyvinylidene difluoride membranes (Amersham Pharmacia Biotech, Piscataway, USA). Then, blocking was performed with 5% skimmed milk in Tris-buffered saline containing 0.1% Tween-20 (TBST) for 1 h at room temperature, and the membranes were probed with primary antibodies as indicated at 4°C overnight, washed with TBST for four times, and subsequently incubated with horseradish peroxidase-conjugated secondary antibody for 45 min. Membranes were washed with TBST for three times and proteins were visualized using an enhanced chemiluminescence detection kit (Millipore, Billerica, USA). For stripping the blot, BlotFresh Western Blot Stripping Reagent (Ver. II) (SignaGen, Gaithersburg, USA) was used according to manufacturer's recommendations. Membranes were washed two times with TBST, and then the blocking and subsequent steps were followed.

Table 1. Primers used for quantitative-polymerase chain reaction

Gene	Forward primer (5′→3′)	Reverse primer (5′→3′)	Size (bp)
MMP2	GTCCAGAGGCAATGCAGTGGG	TCACTAGGCCAGCTGGTTGGTTC	100
MMP9	GCGGTGATTGACGACGCCT	ATACCCGTCTCCGTGCTCCG	135
GAPDH	GTTAGGAAAGCCTGCCGGTG	GCATCACCCGGAGGAGAAATC	118

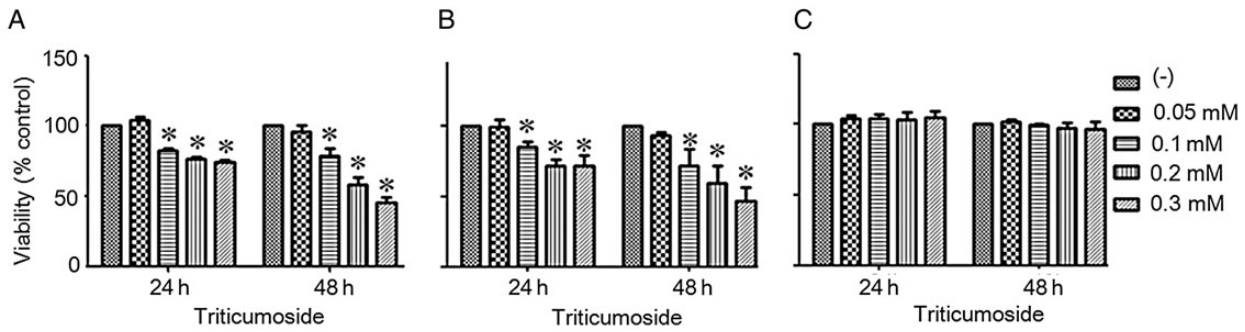

Figure 2. Triticumoside inhibits lung cancer cell viability without causing cytotoxicity to normal HEK293 cells Cells were cultured in 48-well plates and exposed to indicated concentrations of triticumoside for 24 and 48 h. Cell viability of A549 (A), Calu-6 (B), and HEK293 (C) cells was analyzed by CCK-8 assay. Bars represent the mean ± SEM of experiments performed in triplicate. *$P < 0.05$ vs (−).

Statistical analysis

All values are presented as the mean ± SEM. Statistical significance was determined using the Student's *t*-test. *P* values lower than 0.05 were considered statistically significant.

Results

Triticumoside induces cytotoxicity in NSCLC A549 cells

To observe the effect on viability of the cells upon triticumoside treatment, we performed cytotoxicity test using the CCK-8 kit in the cells

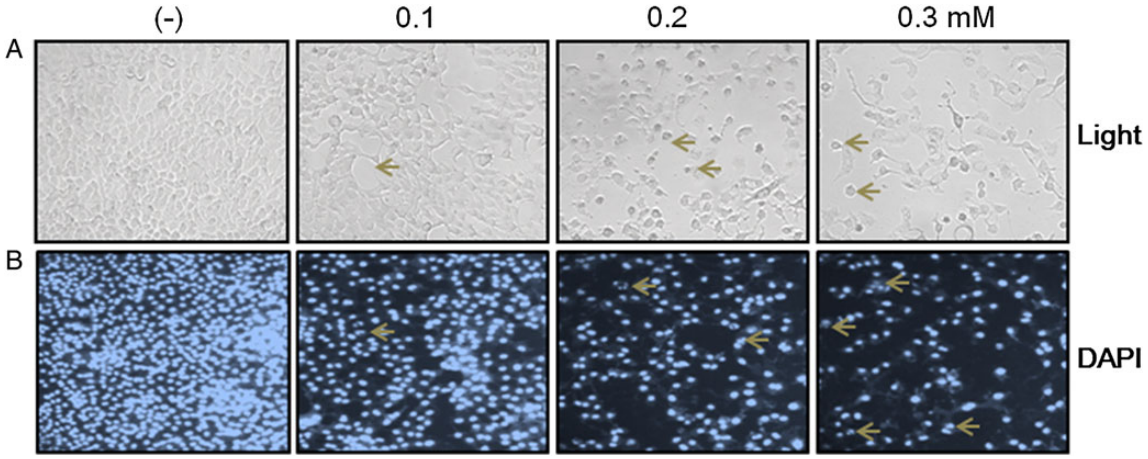

Figure 3. Effect of triticumoside on morphology of A549 cells (A) Cells were cultured in 48-well plates for 48 h with or without various doses of triticumoside and change in morphological features of cells was visualized using an inverted microscope (magnification ×10). (B) After 48 h of culture in 48-well dishes in the presence or absence of triticumoside at indicated concentrations (as described in Materials and Methods), the cells were stained by DAPI and visualized using a fluorescence microscope (magnification ×10).

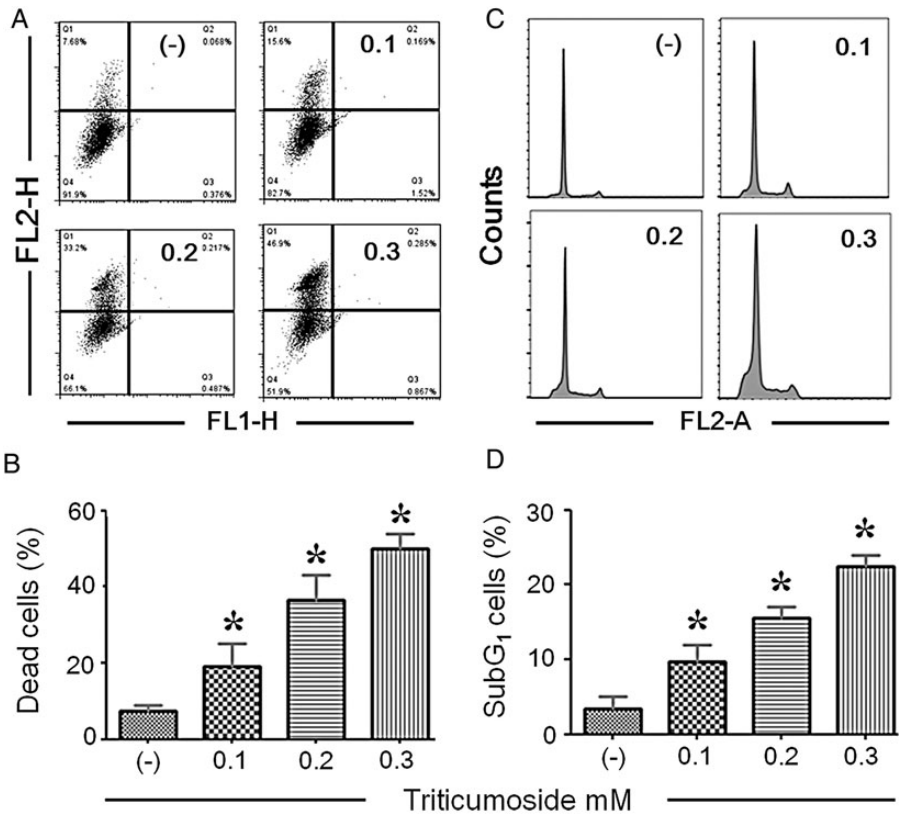

Figure 4. Effect of triticumoside on apoptosis induction and cell cycle regulation in A549 cells (A) Cells were treated with or without mentioned doses of triticumoside for 48 h and the presence of apoptotic cells was analyzed by flow cytometry using annexin-V-FITC and PI staining. (B) Bars represent the mean + SEM of three experiments. (C) Cells were treated with or without indicated concentrations of triticumoside for 24 h. Then, cells were harvested, fixed, and stained with PI. Cell cycle analysis was performed by flow cytometry. (D) Bars shown are mean ± SEM of three independent experiments. **P* < 0.05 vs (–).

treated with or without various doses of triticumoside at different time points. As shown in **Fig. 2A,B**, triticumoside substantially enhanced the death of the NSCLC A549 and Calu-6 cells in time- and dose-dependent manner. At 0.3 mM, triticumoside caused ~20% and 50% cell death at 24 and 48 h, respectively. However, no significant cell death was observed at mentioned doses of triticumoside in normal HEK293 human cells (**Fig. 2C**), suggesting that triticumoside specifically renders cytotoxicity toward cancer cells.

Microscopic examination of NSCLC A549 cell morphology upon triticumoside treatment

To confirm the results obtained from CCK-8 assay and to check the morphological patterns of the cells after triticumoside treatment, we employed phase contrast and fluorescence microscopy technique to observe the cells after triticumoside treatment for 48 h. After being treated with various concentrations of triticumoside for 48 h, a significant proportion of cells showed cytoplasmic shrinkage and cell rounding, and the cell density was reduced in a dose-dependent manner (**Fig. 3A,B**). **Figure 3B** also indicated that untreated cells did not appear to have cytoplasmic shrinkage and had homogenous nuclei, whereas triticumoside-treated cells showed condensed nuclei and apoptotic bodies.

Apoptosis analysis by flow cytometry using annexin-V-FITC and PI staining

As we observed significant cell death in triticumoside-treated cells, we performed flow cytometric analysis after annexin-V-FITC and PI staining to measure apoptotic cell death. NSCLC A549 cells were incubated in the presence or absence of various doses of triticumoside for 48 h, followed by analysis of the apoptotic cells. As shown in

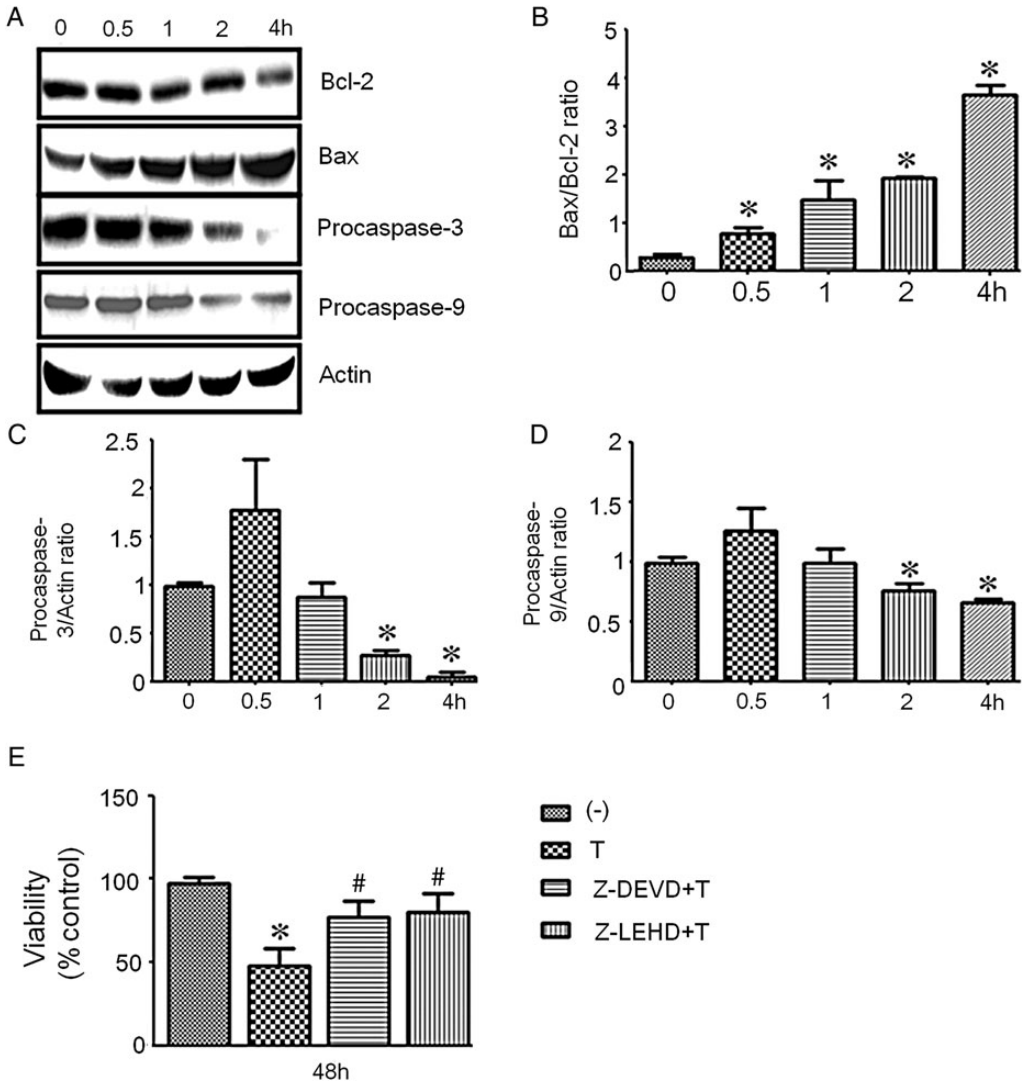

Figure 5. Effect of triticumoside on expression of apoptosis-associated proteins (A) Cells were cultured in 10-cm dishes in the presence or absence of triticumoside for indicated time. Then, cells were washed two times with ice-cold PBS and lysed using RIPA buffer. Then, equal amount of proteins was analyzed using western blotting technique (as described in Materials and Methods) for the expression of indicated proteins. Each membrane was also probed with anti-actin antibody to confirm equal loading of protein. (B) Bars represent the ratio of Bax/Bcl-2 band intensities. (C) Bars shown are the ratio of procaspase-3/actin band intensities. (D) Bars shown are the ratio of procaspase-9/actin band intensities. Error bars indicate mean ± SEM of three separate experiments. (E) Cells were treated with 0.3 mM triticumoside and 15 μm caspase inhibitors for 48 h. Then, cell viability was measured using CCK-8 method. Error bars indicate the mean ± SEM of three separate experiments. $^{*}P < 0.05$ vs (−); $^{\#}P < 0.05$ vs T. T, triticumoside.

Fig. 4A,B, the percentage of apoptotic cells was increased dose dependently after triticumoside treatment. Furthermore, cell cycle analysis data showed that triticumoside treatment for 24 h substantially enhanced sub-G1 cell population in a dose-dependent manner. As shown in **Fig. 4C,D**, 1.9% of cells were apoptotic in untreated cells, while the percentage of cells in sub-G1 was increased up to 23.4% following triticumoside treatment. These data suggest that triticumoside suppresses the growth of NSCLC A549 cells and induces apoptosis, implying its anticancer potential against human cancers.

Triticumoside affects the levels of apoptosis-associated proteins in NSCLC A549 cells

To elucidate that triticumoside-related apoptosis was due to changes of expression in apoptosis-related proteins, cells were exposed to 0.3 mM triticumoside for 0, 0.5, 1, 2, and 4 h, and then the levels of apoptosis-associated proteins were analyzed by western blotting technique. As shown in **Fig. 5A**, triticumoside increased the level of Bax (pro-apoptotic protein), but it reduced the levels of procaspase-3/9 and Bcl-2 (antiapoptotic protein). Similarly, Bax/Bcl-2 ratio of band intensities of specific bands at **Fig. 5A** was also significantly upregulated in a time-dependent manner. Furthermore, the ratios of procaspase-3/actin and procaspase-9/actin were markedly reduced after 2 h of triticumoside treatment (**Fig. 5C,D**). Importantly, when the cells were treated with caspase inhibitors in the presence of 0.3 mM triticumoside for 48 h, the cell viability was increased when compared with control cells (**Fig. 5E**).

Triticumoside inhibits migration of NSCLC A549 cells through inhibition of MMP2/9 expression

We further sought to examine whether triticumoside suppresses NSCLC A549 cell motility. To do so, would healing assay was used. Results showed that 0.05 mM triticumoside significantly inhibited the cell migratory potential after 18 h incubation when compared with untreated cells (**Fig. 6A**). We also sought to investigate whether there was a change in the molecular pathways mediating these functions. As several reports have indicated that MMPs are

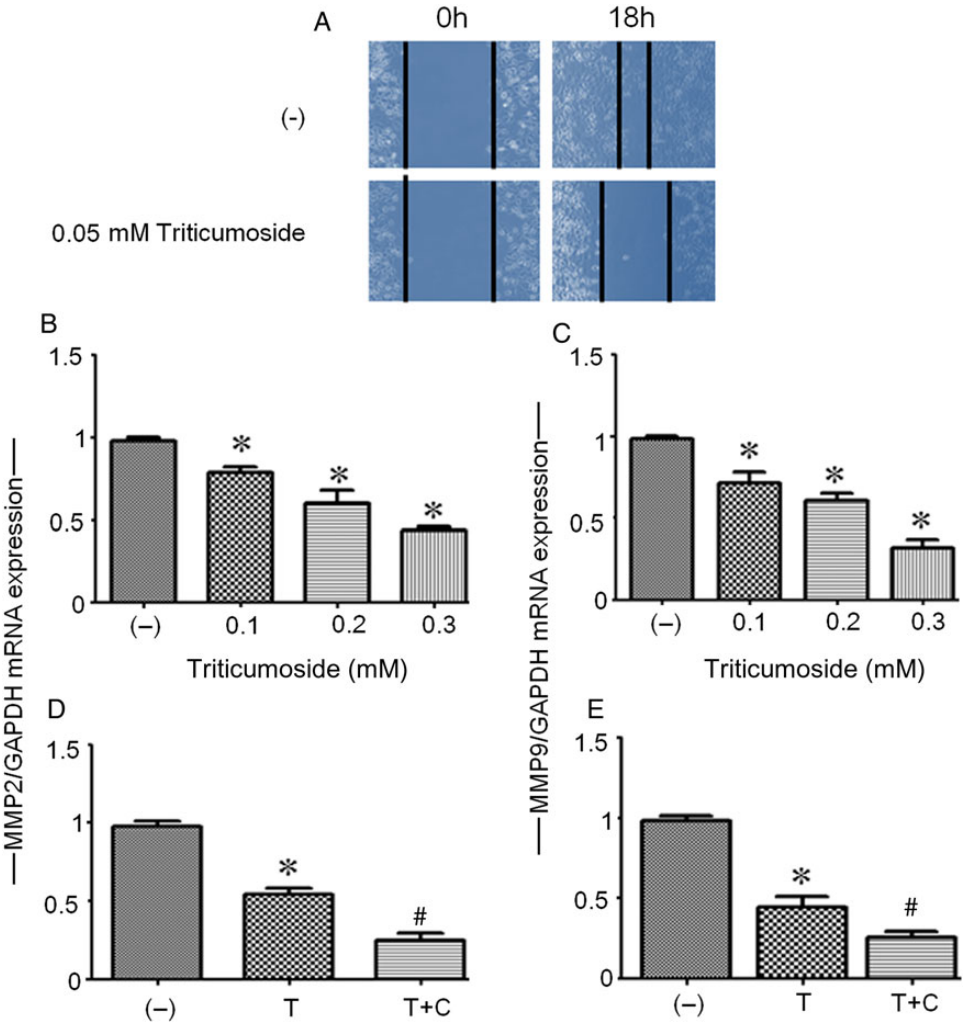

Figure 6. Effect of triticumoside on A549 cells migration (A) Migration of cells was analyzed using μ-dish culture inserts as mentioned in Materials and Methods. Images were acquired at 0 or 18 h of the wells treated with or without triticumoside (magnification ×10). Images shown represent the experiments performed in triplicate. RNA was isolated from the cells using TRIzol method treated with or without indicated doses of triticumoside for 6 h, and reverse transcribed to cDNA using Super Script™ III kit. Then, MMP2 (B) and MMP9 (C) mRNA expressions were analyzed by quantitative-PCR method. The cells were treated with triticumoside (0.3 mM) for 6 h following 1 h preincubation with curcumin (0.03 mM). Then MMP2 (D) and MMP9 (E) mRNA expressions were analyzed by quantitative-PCR method. Error bars indicate mean ± SEM of experiments performed in triplicate. *$P < 0.05$ vs (–); #$P < 0.05$ vs T. T, triticumoside and C, curcumin.

the key molecules associated with migration and invasion of cancer cells, we checked the levels of MMP2/9 expression in the cells exposed to vehicle only or triticumoside. As shown in **Fig. 6B,C**, triticumoside significantly inhibited MMP2/9 expression in a dose-dependent manner, suggesting that triticumoside modulates the expression of MMPs to inhibit cancer cell metastasis. In order to confirm these results, we utilized curcumin as MMP2/9 inhibitor [13] and performed gene expression analysis after triticumoside treatment following preincubation with curcumin. Results indicated that pretreatment with curcumin strongly inhibits MMP2/9 expression in triticumoside-treated cells (**Fig. 6D,E**). These results suggest that similar to curcumin, triticumoside is an inhibitor of MMP2/9 expression in cancer cells.

Discussion

This study has beneficial findings in terms of lung cancer treatment. Firstly, a novel compound isolated from TA, triticumoside, could be applied as a pharmacological anticancer agent to induce NSCLC A549 cell apoptosis, and secondly, it could suppress their migration.

This is the new finding about the role of TA, and particularly its active compound, triticumoside, in cancer cell apoptosis and migration. Many patients develop tumor metastasis and show poor prognosis when compared with the patients with no metastasis [14]. Therefore, adequate therapy to block cancer cells proliferation and migration has become an area of deep research interest [14]. Our study shows that triticumoside causes significant and growth inhibition in lung cancer cells. Light and fluorescent microscopy using DAPI staining showed that it caused morphological changes, including rounding of cells, shrinkage, and nuclear condensation in the cells. Consistent with our results, a previous report has shown that luteolin causes distinctive morphological changes in 786-O renal cancer cells, leading to their apoptosis [15]. Additionally, the decreased procaspase-3/9 and Bcl-2 levels and enhanced Bax levels and sub-G1 proportion of cells suggested that the growth inhibition caused by triticumoside was due to apoptosis. Notably, both caspase-3 and caspase-9 inhibitors attenuated the apoptosis induced by triticumoside. Therefore, the activation of caspase-dependent pathway seemed to be involved in NSCLC A549 cell death caused by triticumoside. Similar to our results, a recent study also showed that *Tetrastigma hemsleyanum* extract induces apoptosis in liver cancer cells via modulation of mitochondrial protein expression and cell cycle arrest [16]. In line with our findings, another study showed that matrine, a component of the extracts from the dry roots of *Sophora flavescens*, upregulates Bax, inhibits Bcl-2 levels, and activates caspase-3 cascade, leading to apoptosis in rat osteosarcoma UMR-108 cells [17]. Furthermore, triticumoside (0.05 mM) at nontoxic dose significantly inhibited migration of the cells as demonstrated by wound healing assay. During cancer cell metastasis, MMPs play crucial role in breaking tissue barrier. Among MMPs, MMP2 and MMP9 are known to be closely related to cancer cell invasion and metastasis [18,19]. In our study, we found that triticumoside significantly suppressed MMP2/9 mRNA expression in a dose-dependent manner. In line with our results, one study showed that crude extract of *Euphorbia formosana* inhibits MMP2/9 expression in DU145 human prostate cancer cells to inhibit their migration, suggesting that the extract acts as an antimetastatic agent [20].

Taken together, these data show that triticumoside may be a natural anticancer molecule that inhibits NSCLC A549 cell proliferation and migration. Additional *in vivo* studies are needed to confirm the signaling pathways associated with anticancer effects of triticumoside.

Funding

This research was supported by a grant from the Basic Science Research Program through the National Research Foundation of Korea (NRF) funded by the Ministry of Education, Science and Technology (No. 2015R1D1A3A01020625).

References

1. Lee SH, Lee JS, Lee EJ, Min KH, Hur GY, Lee SH, Lee SY, *et al*. Serum reactive oxygen species modulator 1 (Romo1) as a potential diagnostic biomarker for non-small cell lung cancer. *Lung Cancer* 2014, 85: 175–181.
2. Hwang KE, Na KS, Park DS, Choi KH, Kim BR, Shim H, Jeong ET, *et al*. Apoptotic induction by simvastatin in human lung cancer A549 cells via Akt signaling dependent down-regulation of surviving. *Invest New Drugs* 2011, 29: 945–952.
3. Lee SH, Lim SW, Lee YM, Lee HS, Kim DK. Polysaccharide isolated from *Triticum aestivum* stimulates insulin release from pancreatic cells via the ATP-sensitive K^+ channel. *Int J Mol Med* 2009, 29: 913–919.
4. Lee SH, Lee YM, Lee HS, Kim DK. Anti-oxidative and anti-hyperglycemia effects of *Triticum aestivum* wheat sprout water extracts on the streptozotocin-induced diabetic mice. *Kor J Pharmacogn* 2009, 40: 408–414.
5. Arya P, Kumar M. Chemoprevention by *Triticum aestivum* of mouse skin carcinogenesis induced by DMBA and croton oil—association with oxidative status. *Asian Pac J Cancer Prev* 2011, 12: 143–148.
6. Hussain A, Gheewala TM, Vas AJ, Shah K, Goala P, Khan S, Hinduja S, *et al*. Growth inhibitory and adjuvant therapeutic potential of aqueous extract of *Triticum aestivum* on MCF-7 and HeLa cells. *Exp Oncol* 2014, 36: 9–16.
7. Lee SH, Lim SW, Lee YM, Hur JM, Lee HS, Kim DK. Anti-diabetic effects of *Triticum aestivum* L. water extracts in db/db mice as an animal model of diabetes mellitus type II. *Kor J Pharmacogn* 2010, 41: 282–288.
8. Lee SH, Xin M, Luyen BTT, Cha JY, Im JY, Kwon SU, Lim SW, *et al*. Inhibitory effect of *Triticum aestivum* ethanol extract on lipid accumulation in 3T3-L1 preadipocytes. *Yakhak Hoeji* 2011, 55: 478–484.
9. Lee SH, Lim SW, Lee YM, Lee SH, Kim DK. Inhibitory effects of *Triticum aestivum* L. extracts on liver lipid accumulation in high fat-fed mice. *Kor J Pharmacogn* 2011, 42: 309–316.
10. Luyen BTT, Thao NP, Tai BH, Lim JY, Ki HH, Kim DK, Lee YM, *et al*. Chemical constituents of Triticum aestivum and their effects on adipogenic differentiation of 3T3-L1 preadipocytes. *Arch Pharm Res* 2015, 38: 1011–1018.
11. Poudel B, Nepali S, Xin M, Ki HH, Kim YH, Kim DK, Lee YM. Flavonoids from *Triticum aestivum* inhibit adipogenesis in 3T3-L1 cells through up-regulation of the insig pathway. *Mol Med Rep* 2015, 12: 3139–3145.
12. Luyen BTT, Tai BH, Thao NP, Cha JY, Lee YM, Kim YH. A new phenolic component from *Triticum aestivum* sprouts and its effects on LPS-stimulated production of nitric oxide and TNF-α in RAW 264.7 cells. *Phytother Res* 2014, 28: 1064–1070.
13. Chen Q, Gao Q, Chen K, Wang Y, Chen L, Li X. Curcumin suppresses migration and invasion of human endometrial carcinoma cells. *Oncol Lett* 2015, 10: 1297–1302.
14. Cheng WY, Chiao MT, Liang YJ, Yang YC, Shen CC, Yang CY. Luteolin inhibits migration of human glioblastoma U-87 MG and T98G cells through downregulation of Cdc42 expression and PI3K/AKT activity. *Mol Biol Rep* 2013, 40: 5315–5326.
15. Ou YC, Kuan YH, Li JR, Raung SL, Wang CC, Hung YY, Chen CJ. Induction of apoptosis by luteolin involving Akt inactivation in human 786-O renal cell carcinoma cells. *Evid Based Complement Alternat Med* 2013, 2013: 109105.

16. Peng X, Zhuang DD, Guo QS. Induction of S phase arrest and apoptosis by ethyl acetate extract from *Tetrastigma hemsleyanum* in human hepatoma $HepG_2$ cells. *Tumor Biol* 2015, 36: 2541–2550.
17. Yan F, Liu Y, Wang W. Matrine inhibited the growth of rat osteosarcoma UMR-108 cells by inducing apoptosis in a mitochondrial-caspase-dependent pathway. *Tumor Biol* 2013, 34: 2135–2140.
18. Poudel B, Kim DK, Ki HH, Kwon YB, Lee YM, Kim DK. Downregulation of ERK signaling impairs U2OS osteosarcoma cell migration in collagen matrix by suppressing MMP9 production. *Oncol Lett* 2014, 7: 215–218.
19. Poudel B, Lee YM, Kim DK. DDR2 inhibition reduces migration and invasion of murine metastatic melanoma cells by suppressing MMP2/9 through ERK/NF-κB pathway. *Acta Biochim Biophys Sin (Shanghai)* 2015, 47: 292–298.
20. Yang JL, Lin JH, Weng SW, Chen JC, Yang JS, Amagaya S, Wood WG, *et al*. Crude extract of *Euphorbia formosana* inhibits the migration and invasion of DU145 human prostate cancer cells: the role of matrix metalloproteinase-2/9 inhibition via the MAPK signaling pathway. *Mol Med Rep* 2013, 7: 1403–1408.